Science Advances
AAAS

Supplementary Materials for

INF2 mutations cause kidney disease through a gain-of-function mechanism

Balajikarthick Subramanian *et al.*

Corresponding author: Balajikarthick Subramanian, bsubram1@bidmc.harvard.edu;
Martin R. Pollak, mpollak@bidmc.harvard.edu

Sci. Adv. **10**, eadr1017 (2024)
DOI: 10.1126/sciadv.adr1017

This PDF file includes:

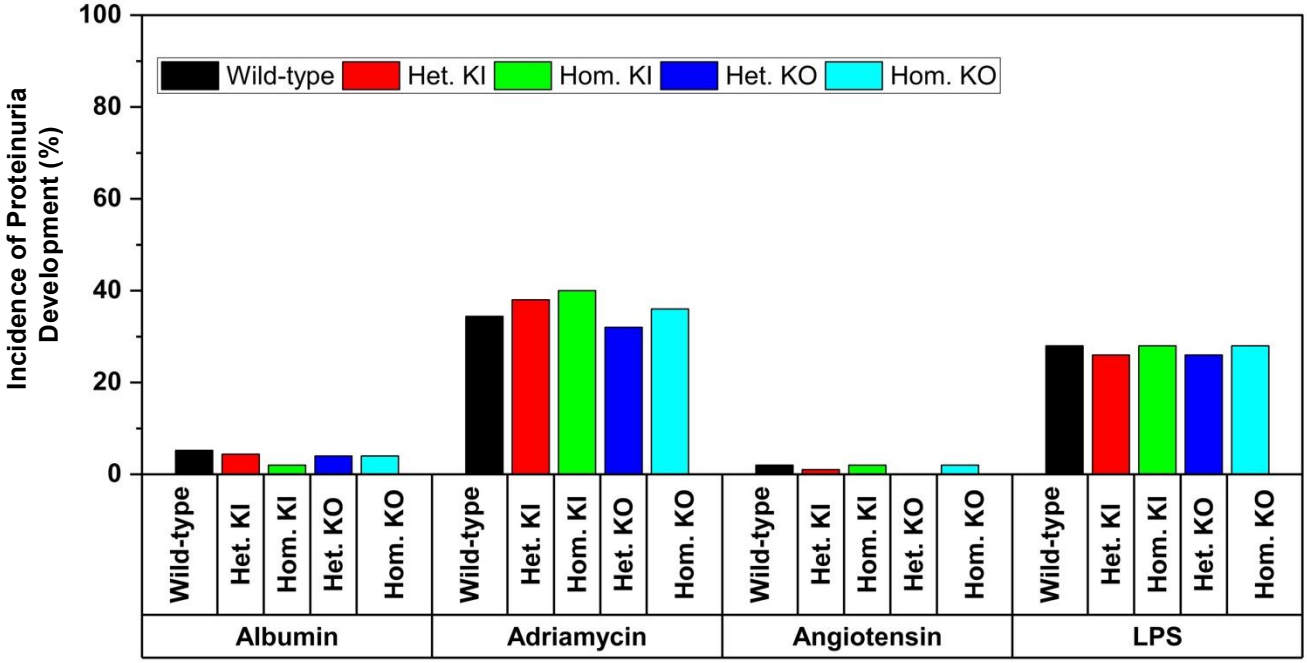

Figure S1. Incidence of proteinuria development among INF2 mouse models subjected to various podocyte stressors. INF2 mouse models were exposed to albumin, adriamycin, angiotensin, and LPS and then evaluated for proteinuria development. The percent count of mice exhibiting proteinuria at Day 5 post-injury was recorded. None of the stressors were able to induce disease in INF2 mouse models selectively.

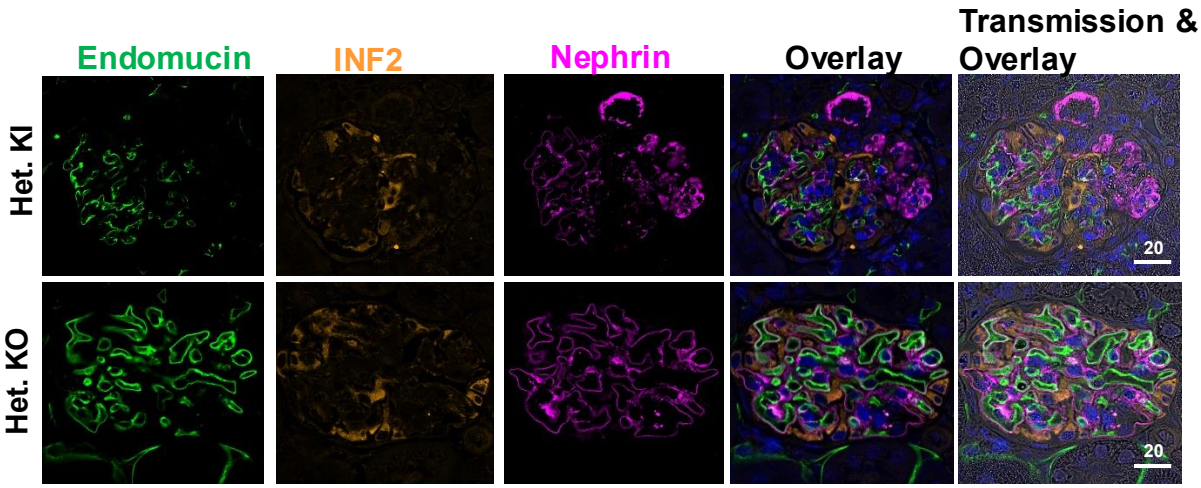

Figure S2. **Glomerular marker protein analysis.** PAN-stressed heterozygous knock-in and heterozygous knock-out mice kidney sections were stained for glomerular marker proteins: Nephrin (Purple); Endomucin (Green); INF2 (Orange). Focal sclerotic lesions were present in PAN-stressed heterozygous knock-in mice (white arrow). Scale bar, 10 μm

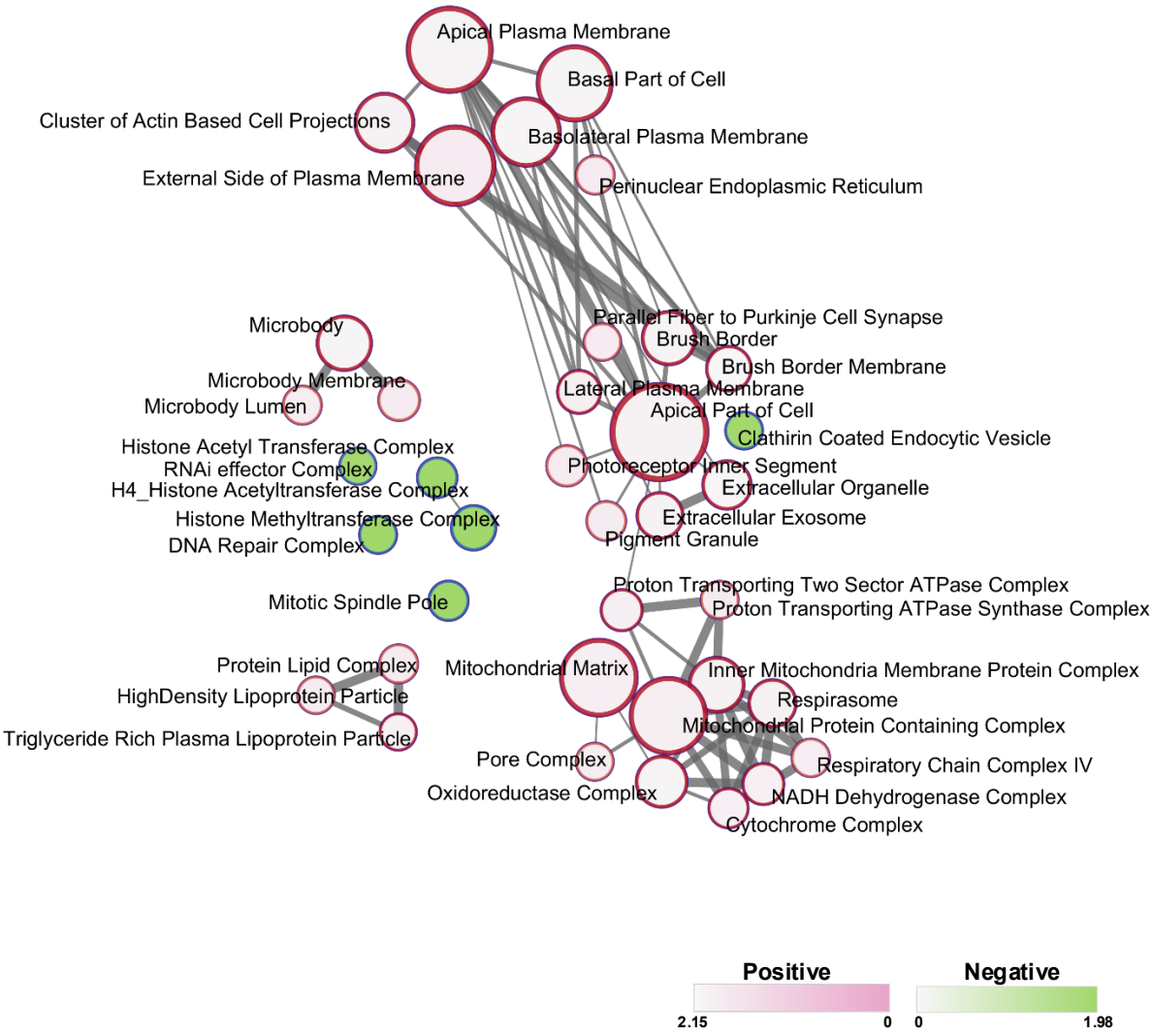

Figure S3. Gene Set Enrichment Network. Pathways that were significantly enriched in the comparison between the PAN-stressed heterozygous knock-in and heterozygous knock-out condition were plotted as a network in the Cytoscape application. Color nodes indicate the upregulated and down-regulated pathways. Connecting lines indicate the gene overlap between pathways. Nodes were manually laid out to form a clearer picture of gene overlaps between pathways. Individual node labels indicate the enriched pathway.

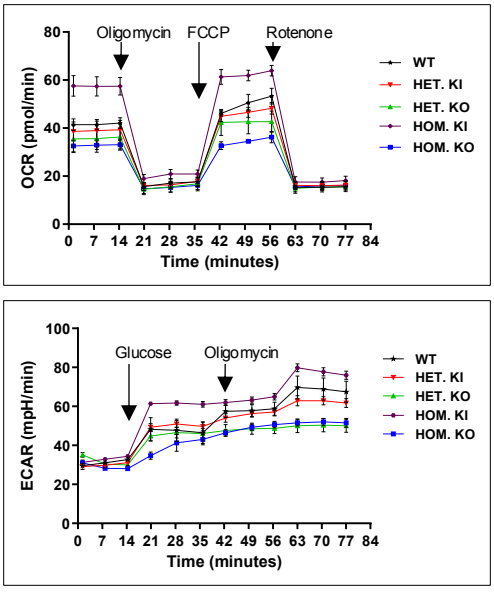

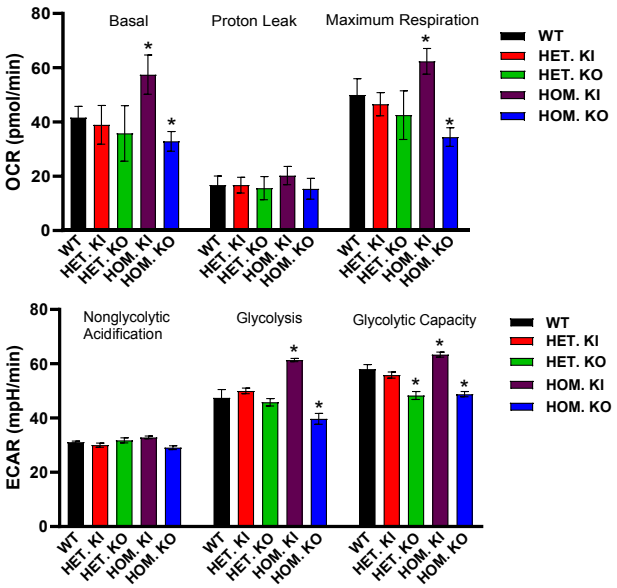

Figure S4. Mitochondrial bioenergetics in podocytes. Seahorse analyses were conducted in basal conditions of podocytes derived from INF2 knock-in and knockout models. (a) oxygen consumption rate (OCR) and (b) basal respiration, proton leak, and maximum respiration in podocytes. (c) extracellular acidification rate (ECAR) and (d) non-glycolytic acidification, glycolysis, and glycolytic capacity in podocytes. Statistical analyses were conducted by comparison with the wild-type group. * $p<0.05$.

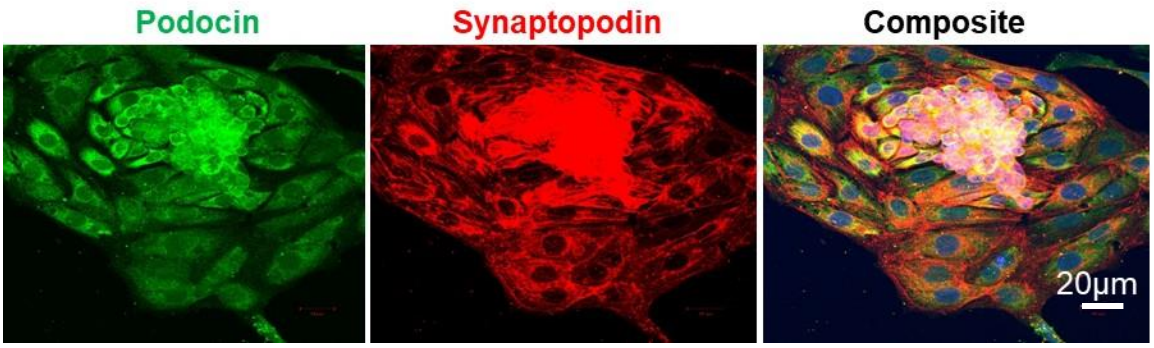

Figure S5. Immunofluorescence analysis of podocytes derived from organoids. The outgrown cells were stained for podocyte marker proteins podocin and synaptopodin, and the nucleus was counterstained using DAPI.

y Table 1 Gene sets enriched in Het-KI phenotype

Gene Sets	Size	NES	FDR q-value
GOCC_BRUSH_BORDER_MEMBRANE	72	2.16	0
GOCC_EXTRACELLULAR_ORGANELLE	96	2.05	0
GOCC_BASOLATERAL_PLASMA_MEMBRANE	229	2	0.001
GOCC_BASAL_PART_OF_CELL	274	1.98	0.001
GOCC_MICROBODY	136	1.98	0.001
GOCC_APICAL_PLASMA_MEMBRANE	341	1.97	0.001
GOCC_OXIDOREDUCTASE_COMPLEX	112	1.97	0.001
GOCC_BRUSH_BORDER	128	1.92	0.001
GOCC_EXTRACELLULAR_EXOSOME	80	1.92	0.001
GOCC_RESPIRASOME	88	1.92	0.001
GOCC_APICAL_PART_OF_CELL	421	1.89	0.002
GOCC_INNER_MITOCHONDRIAL_MEMBRANE_PROTEIN_ COMPLEX	139	1.84	0.004
GOCC_CLUSTER_OF_ACTIN_BASED_CELL_PROJECTIONS	166	1.84	0.004
GOCC_NADH_DEHYDROGENASE_COMPLEX	47	1.81	0.006
GOCC_LATERAL_PLASMA_MEMBRANE	60	1.78	0.009
GOCC_CYTOCHROME_COMPLEX	35	1.78	0.009
GOCC_TRIGLYCERIDE_RICH_PLASMA_LIPOPROTEIN_PARTICLE	15	1.76	0.011
GOCC_MITOCHONDRIAL_PROTEIN_CONTAINING_COMPLEX	283	1.74	0.013
GOCC_MITOCHONDRIAL_MATRIX	285	1.73	0.015
GOCC_PROTON_TRANSPORTING_TWO_SECTOR_ATPASE_ COMPLEX	47	1.67	0.028
GOCC_RESPIRATORY_CHAIN_COMPLEX_IV	23	1.66	0.034
GOCC_PORE_COMPLEX	20	1.65	0.035
GOCC_MICROBODY_LUMEN	27	1.65	0.033
GOCC_HIGH_DENSITY_LIPOPROTEIN_PARTICLE	16	1.62	0.045
GOCC_PROTEIN_LIPID_COMPLEX	27	1.61	0.049
GOCC_PIGMENT_GRANULE	32	1.61	0.051
GOCC_MICROBODY_MEMBRANE	45	1.56	0.08
GOCC_PERINUCLEAR_ENDOPLASMIC_RETICULUM	26	1.56	0.081
GOCC_PROTON_TRANSPORTING_ATP_SYNTHASE_COMPLEX	20	1.55	0.081
GOCC_EXTERNAL_SIDE_OF_PLASMA_MEMBRANE	303	1.55	0.08
GOCC_PARALLEL_FIBER_TO_PURKINJE_CELL_SYNAPSE	17	1.54	0.086
GOCC_PHOTORECEPTOR_INNER_SEGMENT	42	1.53	0.091
GOCC_RIBOSOMAL_SUBUNIT	193	1.49	0.134
GOCC_MICROVILLUS	85	1.49	0.131
GOCC_CELL_PROJECTION_MEMBRANE	260	1.49	0.129
GOCC_TRICARBOXYLIC_ACID_CYCLE_ENZYME_COMPLEX	20	1.47	0.149
GOCC_APICOLATERAL_PLASMA_MEMBRANE	22	1.47	0.146
GOCC_ENDOPLASMIC_RETICULUM_GOLGI_INTERMEDIATE_ COMPARTMENT_MEMBRANE	16	1.46	0.161
GOCC_CYTOSOLIC_LARGE_RIBOSOMAL_SUBUNIT	62	1.44	0.173
GOCC_APICAL_JUNCTION_COMPLEX	129	1.44	0.174
GOCC_PROTON_TRANSPORTING_TWO_SECTOR_ATPASE_ COMPLEX_CATALYTIC_DOMAIN	16	1.44	0.171
GOCC_VACUOLAR_PROTON_TRANSPORTING_V_TYPE_ATPASE _COMPLEX	23	1.43	0.173
GOCC_CATENIN_COMPLEX	16	1.43	0.17
GOCC_MONOATOMIC_ION_CHANNEL_COMPLEX	153	1.43	0.169
GOCC_LARGE_RIBOSOMAL_SUBUNIT	119	1.43	0.167
GOCC_CYTOSOLIC_RIBOSOME	123	1.42	0.183
GOCC_PROTON_TRANSPORTING_V_TYPE_ATPASE_COMPLEX	27	1.41	0.186
GOCC_TRANSPORTER_COMPLEX	258	1.41	0.183
GOCC_HIPPOCAMPAL_MOSSY_FIBER_TO_CA3_SYNAPSE	42	1.41	0.182
GOCC_SMALL_RIBOSOMAL_SUBUNIT	79	1.4	0.193
GOCC_CYTOSOLIC_SMALL_RIBOSOMAL_SUBUNIT	44	1.39	0.205
GOCC_TIGHT_JUNCTION	114	1.39	0.208
GOCC_PHOTORECEPTOR_OUTER_SEGMENT	52	1.38	0.214
GOCC_CATION_CHANNEL_COMPLEX	100	1.36	0.252
GOCC_PROTON_TRANSPORTING_TWO_SECTOR_ATPASE_ COMPLEX_PROTON_TRANSPORTING_DOMAIN	21	1.36	0.25